# *Kinetic Prefactors of Reactions on Solid Surfaces*





| | |
|---|---|
| **Citation** | Campbell, C. T., Árnadóttir, L., & Sellers, J. R. (2013). Kinetic Prefactors of Reactions on Solid Surfaces. Zeitschrift für Physikalische Chemie, 227, 1435-1454. doi:10.1524/zpch.2013.0395 |
| **DOI** | 10.1524/zpch.2013.0395 |
| **Publisher** | Walter de Gruyter GmbH |
| **Version** | Version of Record |
| **Citable Link** | http://hdl.handle.net/1957/47888 |
| **Terms of Use** | http://cdss.library.oregonstate.edu/sa-termsofuse |

Z. Phys. Chem. **227** (2013) 1435–1454 / **DOI** 10.1524/zpch.2013.0395


# Kinetic Prefactors of Reactions on Solid Surfaces

By Charles T. Campbell[1,*], Líney Árnadóttir[2], and Jason R. V. Sellers[1]

[1] Department of Chemistry, University of Washington, Seattle, WA 98195-1700, USA
[2] School of Chemical, Biological and Environmental Engineering, Oregon State University, Corvallis, OR 97331-2702, USA

(Received January 31, 2013; accepted in revised form April 29, 2013)
(Published online August 5, 2013)

***Surface Reactions / Adsorbate / Kinetics / Kinetic Prefactors / Transition State Theory***

Adsorbed molecules are involved in many reactions on solid surfaces that are of great technological importance. As such, there has been tremendous effort worldwide to learn how to theoretically predict rates for reactions involving adsorbed molecules. Theoretical calculations of rate constants require knowing both their activation energy and prefactor. Recent advances in *ab initio* computational methods (*e.g.*, density functional theory with periodic boundary conditions and van der Waals corrections) promise to soon provide activation energies for surface reactions with sufficient accuracy to have real predictive ability. However, to predict reaction rates, we also need accurate predictions of prefactors. We recently discovered that the standard entropies of adsorbed molecules ($S^0_{ad}$) linearly track the entropy of the gas-phase molecule at the same temperature ($T$), such that $S^0_{ad}(T) = 0.70\, S^0_{gas}(T) - 3.3\,\mathrm{R}$ (R = the gas constant), with a standard deviation of only 2 R over a range of 50 R. This correlation, which applies only to conditions where their surface residence times are shorter than $\sim 1000$ s, provides a powerful new method for estimating the partition functions for adsorbates and the kinetic prefactors for their reactions. For desorption, we show that the prefactors obtained with DFT using transition state theory (TST) and the harmonic oscillator approximation to get the partition function predicts prefactors for desorption that are of order $10^3$ times larger than experimental values while our approach gives much better estimates. We also explore the applications of this approach to estimate prefactors within TST for the main classes of adsorbate reactions: desorption, diffusion, dissociation and association, and discuss its limitations. We discuss general issues associated with applying TST to rate laws and multi-step mechanisms in surface chemistry, and argue that rates of adsorbate reactions which are often taken to be proportional to coverage ($\theta$) might better be taken as proportional to $\theta/(1-\theta)$ (unless the adsorbate forms islands), to account for the configurational entropy or excluded volume effects on the adsorbate's chemical potential.

## 1. Introduction

Chemical reactions on solid surfaces play a central role in many technologies that will be crucial for our energy and environmental future, including the production and use of solar cells, catalysts for clean fuels and chemicals production and pollution cleanup,

* Corresponding author. E-mail: campbell@chem.washington.edu

photocatalysts, fuel cells, batteries, sorbents and solid reactants. They are also critical to a number of other technologies including microelectronics, computer chips, chemical and biochemical sensors, prosthetic medical devices, reflective and protective coatings, optical, electro-optic and opto-electric devices and adhesives. Thus, there is great motivation to learn how to accurately predict rate constants for the elementary steps that occur in chemical reactions on solid surfaces. To this end, there have been decades of outstanding research from both experimental and theoretical perspectives to measure and calculate rate constants for elementary steps on solid surfaces. The calculations have been largely guided by various adaptations of transition state theory (TST) as introduced for simple gas reactions by Eyring and Polanyi [1]. By far the most common current approach for *ab initio* calculations of rate constants for surface reactions involves the use of Density Functional Theory (DFT) with periodic boundary conditions to calculate potential energy surfaces in the most important regions around the minima (reactants and products) and saddle points (transition states). These generally use efficient saddle-point-finding algorithms such as the Nudged Elastic Band (NEB [2]) and Dimer methods [3] to locate the transition state. The harmonic oscillator approximation is generally invoked around these minima and maxima to calculate the partition functions ($q$) of the adsorbed reactants and transition states (except for the transition state for desorption, which is more often a 2D gas) in calculating the rate constant. This is referred to as harmonic transition state theory (HTST) and assumes that all modes of any adsorbed reactant or transition state are vibrations [4].

Our recent discovery of the very high entropies of adsorbed molecules at the temperatures where their desorption equilibria and rates are measured implies that the harmonic approximation grossly underestimates adsorbate partition functions at such temperatures [5]. Here, we explore the implications of this discovery with respect to predicting rate constants for surface reactions, and particularly their preexponential factors, $\nu$, and suggest new approximations for estimating these prefactors which go beyond HTST. We discuss in detail when this new approach will be necessary. We expect that HTST remains valid at temperatures where all the reactants involved in the elementary step have rates of desorption below $10^{-3}$ monolayers/s, which includes a very wide range of important processes.

## 2. Entropies of adsorbed molecules

We recently presented the first extensive tabulation of the experimentally-measured entropies of adsorbed molecules on well-defined surfaces [5]. From this, we found that their standard entropies at the measurement temperature, $S^0_{\mathrm{ad}}(T)$, linearly track the standard entropy of the gas-phase molecule at the same temperature, $S^0_{\mathrm{gas}}(T)$, such that

$$S^0_{\mathrm{ad}}(T) = 0.70\, S^0_{\mathrm{gas}}(T) - 3.3\,\mathrm{R}\,, \tag{1}$$

where R is the ideal gas constant. As shown in Fig. 1, this correlation is essentially independent of the surface material, with a standard deviation of only 2 R over a range of 50 R. These entropies, which are $\sim 2/3$ of the gas entropy, are huge compared to most theoretical predictions. Note that these entropies were measured at temperatures ($T$) such that desorption could be observed (*i.e.*, at $T$ such that the desorption rate was

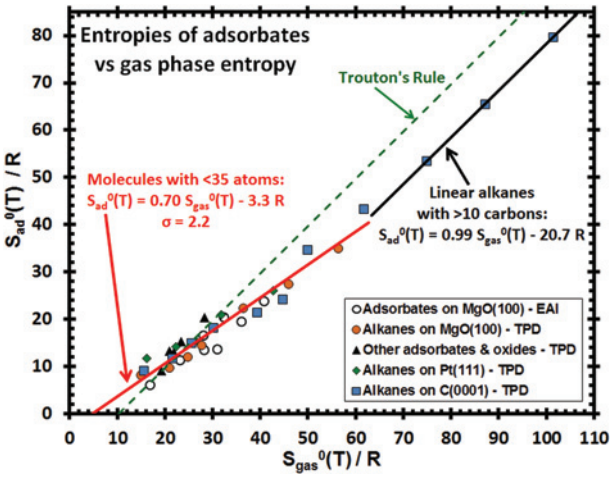


**Fig. 1.** Plot of the standard entropies of molecular adsorbates ($S_{ad}^0$) on several surfaces plotted *vs.* the standard entropy of the gas-phase molecule at the same temperature. For the gas, "standard" refers to the ideal gas at 1 bar pressure. The best linear fits to the data for molecules smaller and larger than 35 atoms are also shown. For comparison, the standard entropies of bulk 3D liquids at the normal boiling point (as estimated by Trouton's Rule) are also shown. From [5].

at least $\sim 10^{-3}$ monolayers (ML) per s), or more appropriately, where the surface residence time $\tau$ is less than $\sim 1000$ s. The actual molecules and substrates associated with each data point in Fig. 1 can be found in the paper where this correlation was originally presented [5].

## 3. Prefactors for desorption

The total instantaneous desorption rate of an adsorbed molecule is typically assumed to be a single-valued function of its coverage ($\theta$) and temperature, $r(\theta, T)$, given by:

$$r(\theta, T) = -\mathrm{d}\theta/\mathrm{d}t = k_{\mathrm{des}}\theta = \nu_{\mathrm{des}} \exp(-E_{\mathrm{des}}(\theta)/\mathrm{R}T)\theta\,, \tag{2}$$

where $k_{\mathrm{des}}$ is the first-order rate constant and $\nu_{\mathrm{des}}$ is the pre-exponential factor, which is typically assumed not to vary with coverage or temperature, and $E_{\mathrm{des}}(\theta)$ is the coverage-dependent desorption activation energy. This approximation will certainly fail in some cases since it neglects the excluded-volume of adsorbates, which is the first correction to a 2D ideal gas model for the adsorbate [6], and since the first-order factor of $\theta$ at the end here should be replaced by $\theta/(1-\theta)$ in the ideal lattice gas approximation (see below), which is closely related to the excluded-volume effect. Much more sophisticated models have been put forth [6–8].

When the activation energy for adsorption is negligible and the sticking probability is near unity, as is usually the case for molecular adsorption, the transition state for desorption is the molecule with its center of mass constricted to lie in a plane parallel to the surface at some distance far enough away from the surface that its interaction

with the surface is negligible for any angle of rotation [9,10]. In this case, the transition state is very well defined. Its entropy ($S^0_{TS,des}$) is identical to that for the gas ($S^0_{gas}$) at the same temperature, except that it is missing one translational degree of freedom (the one perpendicular to the surface):

$$S^0_{TS,des} = S^0_{gas} - S^0_{gas,1D\text{-}trans}\,. \tag{3}$$

The value of $S^0_{gas,1D\text{-}trans}$ for any gas can easily be calculated using statistical mechanics (the Sackur–Tetrode equation) [11], assuming that each translational degree of freedom contributes 1/3 of the total 3D translational entropy. This gives:

$$S^0_{gas,1D\text{-}trans} = (1/3)\left\{S^0_{Ar,298\,K} + \mathrm{R}\ln\left[(m/m_{Ar})^{3/2}(T/298\ \mathrm{K})^{5/2}\right]\right\}, \tag{4}$$

where $m$ is the molar mass of the gas, $m_{Ar}$ is that for argon, and $S^0_{Ar,298\,K}$ is the entropy of Ar gas at 1 bar and 298 K (= 18.6 R). The value of $S^0_{gas}$ can generally be found from standard thermodynamic tables, using the heat capacity to extrapolate to unlisted temperatures.

Within transition state theory, the rate constant for first-order desorption is given by [6,9,10]:

$$k_{des} = (k_B T/h)\left(q^0_{TS}/q^0_i\right)\exp\left(-\Delta E^0_{TS}/k_B T\right), \tag{5}$$

where $q^0_{TS}$ is the partition function for the transition state (omitting motion in the coordinate perpendicular to the surface) and $q^0_i$ is the partition function for the adsorbate. The superscript "0" in both cases means that these are both evaluated about their zero-point energies (*i.e.*, taking all energies relative to the ground state for that species), and $\Delta E^0_{TS}$ is the difference between these two zero-point energies. The desorption prefactor (approximately equal to $(k_B T/h)(q^0_{TS}/q^0_i)$) is given by [12]:

$$\nu_{des} = k_B T/h \exp\left(\Delta S^0_{TS,des}/\mathrm{R}\right) = k_B T/h \exp\left[\left(S^0_{TS,des} - S^0_{ad}\right)/\mathrm{R}\right], \tag{6}$$

where $k_B$ is Boltzmann's constant and $h$ is Planck's constant, and $E_{des}$ is the standard enthalpy of activation. (If one takes the strict definition of activation energy as −R times the slope of ln(rate constant) *vs.* $1/T$, one gets that $E_{des} = -\Delta H^0_{ad}(T) - {}^1\!/_2\mathrm{R}T$ [13], where $\Delta H^0_{ad}(T)$ is the standard enthalpy of adsorption. One also gets an additional factor of e in the expression for $\nu_{des}$ in Eq. (6), which arises from the contribution of $k_B T/h$ to this slope [14], and which we neglect below.) Substitution using Eq. (3) gives:

$$\nu_{des} = k_B T/h \exp\left[\left(S^0_{gas} - S^0_{gas,1D\text{-}trans} - S^0_{ad}\right)/\mathrm{R}\right], \tag{7}$$

where all entropies are for the same temperature $T$ as the measurement of $\nu_{des}$. We show below that if one uses the harmonic oscillator approximation to get $S^0_{ad}$ (*i.e.*, HTST) for this equation, it results in prefactors that are many orders of magnitude too large. We further show that using the empirical correlation of Fig. 1 to get $S^0_{ad}$ gives much, much better results.

Equation (7) can be rearranged to give an expression for calculating $S^0_{ad}$ from an experimental value of $\nu_{des}$:

$$S^0_{ad} = \left(S^0_{gas} - S^0_{gas,1D\text{-}trans}\right) - \mathrm{R}\ln[\nu_{des}h/(k_B T)]\,. \tag{8}$$

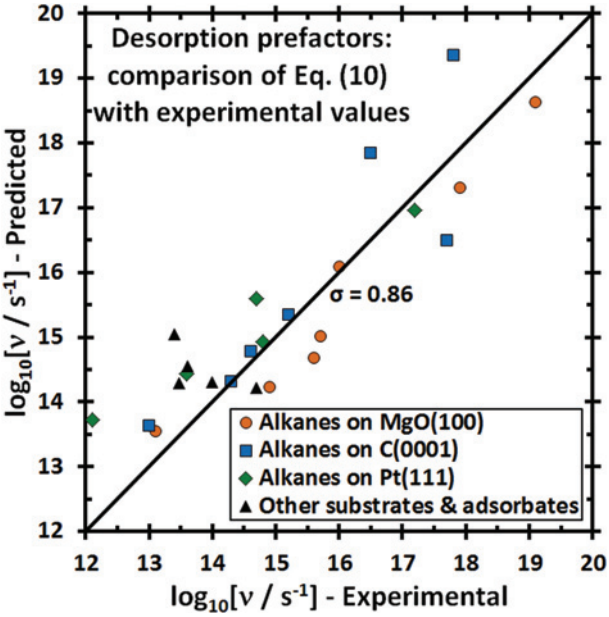


**Fig. 2.** Prefactors for the desorption of molecularly adsorbed species as predicted from the gas-phase entropies using Eq. (9) (which was derived from the linear relationship in Fig. 1 using transition state theory) plotted *vs.* the experimentally measured prefactors. The line shows the expectation based on Eq. (9), which the data fit with a standard deviation in $\log(\nu/s^{-1})$ of 0.86. From [5].

We used this approach to obtain the entropies for many of the points in Fig. 1, but many also were obtained from more direct measurements using equilibrium adsorption isotherms. Note that if we included the neglected factor of e in Eq. (6) mentioned above, all these $S^0_{ad}$ values determined from TPD in Fig. 1 would increase by R, increasing the $y$-intercept in Eq. (1) for $S^0_{ad}$ from $-3.3$ R to $-2.5$ R with no change in slope. However, all of this difference (except 0.2 R) cancels when we then turn around and use these entropies to estimate prefactors using Eq. (6), which is our main focus below. Similarly, the y-intercept for the line in Fig. 1 for alkanes longer than $C_{10}$ would increase from $-20.7$ R to $-19.7$ R.

The entropy correlation of Fig. 1 (Eq. (1)) can be used to estimate $S^0_{ad}$, and this allows for more reliable estimates of prefactors in rate constants for adsorbate reactions using transition state theory than HTST. We have already demonstrated this for the simplest case, desorption after non-activated molecular adsorption with attractive adsorbate–adsorbate interactions, as follows [5]. Substituting Eq. (1) for $S^0_{ad}$ into Eq. (7) gives the prefactor:

$$\begin{aligned}\nu_{des} &= (k_B T/h)\exp\left[\left(0.30S^0_{gas} + 3.3\,\mathrm{R} - S^0_{gas,1D\text{-}trans}\right)/\mathrm{R}\right] \\ &= (k_B T/h)\exp\left\{0.30S^0_{gas}/\mathrm{R} + 3.3 - (1/3)\{18.6 + \ln[(m/m_{Ar})^{3/2}(T/298\,\mathrm{K})^{5/2}]\}\right\},\end{aligned} \tag{9}$$

where $S^0_{gas,1D\text{-}trans}$ can be calculated from Eq. (4). Figure 2 shows a plot of the predictions of Eq. (9) plotted *vs.* experimentally measured desorption prefactors for all the

molecules on single crystals surfaces in Fig. 1 except alkanes longer than $C_{10}$. The predictions agree very well with these experimental prefactors with a standard deviation in $\log(\nu_{des}/s^{-1})$ of only 0.86, confirming the validity of Eq. (9) for estimating prefactors. For alkanes longer than $C_{10}$, the prefactor stays constant at $\sim 10^{19}$ $s^{-1}$ [15,16]. Several discussions of the values for desorption prefactors have been published [10,15–28]. This analysis corresponds to terrace sites. We showed previously that metal adatoms have a desorption prefactor that is $10^5$-fold larger at step edges than at terrace sites on Mo(100), due to the loss of all translational motion except in the one direction along the step edge [27].

There is a huge difference between the prefactor for desorption one gets using Eq. (1) to get $S^0_{ad}$ (which gives Eq. (9)) compared to that obtained using instead the harmonic oscillator approximation to get $S^0_{ad}$ (*i.e.*, HTST), in both cases starting from Eq. (7). For example, consider the case of methanol on Pt(111). We recently measured the prefactor for its desorption at 210 K to be $4 \times 10^{15\pm0.5}$ $s^{-1}$, with a heat of adsorption of $61.2 \pm 2.0$ kJ/mol [29]. Using Eq. (9) gives $\nu_{des} = 1.3 \times 10^{15}$ $s^{-1}$, which agrees within a factor of 3. In contrast, DFT calculations combined with HTST gives a value that is 1000-fold too large. We performed DFT calculations for methanol on Pt(111) using VASP [30–32] with the projector augmented wavefunction (PAW) method [33,34] together with the GGA-PBE and GGA-PW91 [35–37] functionals. The Pt(111) surface consisted of 45 atoms ($3 \times 3$ unit cell, five layers deep) with one methanol per unit cell. During optimization, the top two Pt layers were allowed to relax, and the methanol was found to adsorb with the oxygen atom on the atop site and two carbonic hydrogens pointing towards the surface, in good agreement with earlier DFT results [38]. Then, the frequencies for all the normal vibrational modes of the methanol atoms were calculated for the adsorbed molecule, keeping all the Pt atoms frozen. The calculated frequencies of these vibrations are in excellent agreement with those same previously reported calculations [38] which, however, did not report the six lowest-frequency modes that contribute essentially all of the entropy. In the harmonic approximation, our DFT frequencies give a vibrational partition function at 210 K (evaluated about its zero-point energy) of only $q^0_{vib} = 65$ to 187 , depending on the functional (PBE and PW91, respectively), and an entropy for the adsorbate at 210 K, $S^0_{ad,HO}$ (equal to the sum over all vibrational modes of $R\{(h\nu_i/kT)/[\exp(h\nu_i/kT) - 1] - \ln[1 - \exp(-h\nu_i/kT)]\}$, where $\nu_i$ is the frequency of that mode [11]) of only 77 J/(mol K) (for the PW91 functional, even less for PBE). Using Eqs. (3) and (4) together with gas-phase entropies (obtained by extrapolating from tabulated values at the nearest temperature using tabulated heat capacities, from standard tables [39]) gives an entropy for the transition state for its desorption ($S^0_{TS,des}$) of 177 J/(mol K). Using these two entropies in Eq. (6) gives $\nu_{des} = 7 \times 10^{17}$ $s^{-1}$ or more, which is larger than the experimental value by a factor of 200 or more. *This huge discrepancy arises because the entropy for the adsorbate estimated in this harmonic approximation is at least* 53 J/(mol K) *lower than the value of* 130 J/(mol K) *estimated using Fig. 1 and Eq. (1).* One gets even worse agreement if one estimates the entropy for the adsorbate in the harmonic approximation as $R \ln(q^0_{vib})$, which is essentially what is done in HTST when the prefactor is estimated as $\nu_{des} = (kT/h)(q^0_{TS}/q^0_{vib})$. This gives an entropy of only 44 J/(mol K) for the PW91 functional (even less for PBE) and a prefactor of $4 \times 10^{19}$ $s^{-1}$, $10^4$-fold larger than the experimental value (or $\sim 10^5$-fold larger for PBE).

## 4. Why do adsorbates have such large entropies?

Before we can extend the above approach for estimating prefactors to other classes of surface reactions besides desorption, and before we can even understand how generally valid Eq. (9) is for estimating $\nu_{des}$, we must first examine the origin of the very high entropies of adsorbed molecules and the slope of $\sim 2/3$ seen in Fig. 1. Our qualitative explanation of this has been published [5]. Briefly, the motions of the gas molecule which give rise to most of its entropy are its translations and rotations, and these can be decomposed into their $x$, $y$ and $z$ components. If we assume their entropy is equally divided between $x$, $y$ and $z$ components, with all components of motion in the $x$ and $y$ directions (*e.g.*, $x$ and $y$ translation and helicopter rotations) not changed from the gas, but with all components of motion in the $z$ direction (*e.g.*, $z$ translation and cartwheel rotations) frozen out by the steep interaction potential well in the $z$ direction, we arrive at a proportional relationship with slope 2/3 in Fig. 1. It implies a very weak corrugation of the molecule – surface interaction potential for translational and rotational motions parallel to the surface, with saddle points that are lower than $k_B$T at the measurement temperature, but a steep well for any type of molecular motion perpendicular to the surface. This same model was offered to explain trends in prefactors for alkane desorption [18,19].

The weak corrugation parallel to the surface for polyatomic molecules is probably due to "lattice mismatch" between the surface's lattice constant and the bond lengths within the adsorbate: The farther the molecule extends along the surface, the bigger the fraction of its atoms not fitting in their most stable binding sites [21]. This is the same reason that the activation barrier for diffusion of a small 2D metal islands decreases with island size when the lattice mismatch with the underlying substrate is large [40].

Equation (1) is similar to Trouton's Rule (the entropy of a liquid at the normal boiling point $= S^0_{gas} - 10.3$ R [41]), also plotted in Fig. 1. As seen, adsorbate entropies are nearly as high as liquid entropies. *This is far above what would be expected based on the statistical thermodynamics models most widely applied to adsorbates, the lattice gas and 2D lattice crystal models, which only include vibrational entropy through the harmonic (or harmonic oscillator, HO) approximation. While this is clearly valid at very low temperatures, it dramatically underestimates their entropies at the temperatures of Fig. 1, where the surface residence time is less than* 1000 s. This is not mainly because the 2nd derivatives of energy *vs.* distance at the energy minima are incorrect (as that would lead to much smaller errors), but instead due to the low energies of the next maxima in the potential energy surface (relative to $k_BT$). This is the same reason that the hindered rotation of one methyl group about the C–C axis in gas-phase ethane contributes only low vibrational entropy at low temperature but, when $k_BT$ exceeds the barrier for that methyl rotation, that mode becomes a free rotor; but even when $k_BT$ is only 15% of the barrier, there is already a very large increase in entropy [11]. The large error of the HO approximation in estimating prefactors was recently pointed out for propane desorption from PdO(101) [42].

The most well studied example of a hindered rotor involves the rotation of one methyl group about the C–C axis in gas-phase ethane. Its potential energy ($V$) *vs.* rotational angle ($\varphi$), shown in Fig. 3, is a repeating cosine wave that has a maximum potential barrier of $W$ repeating every 120°. For the generalized hindered rotor, the

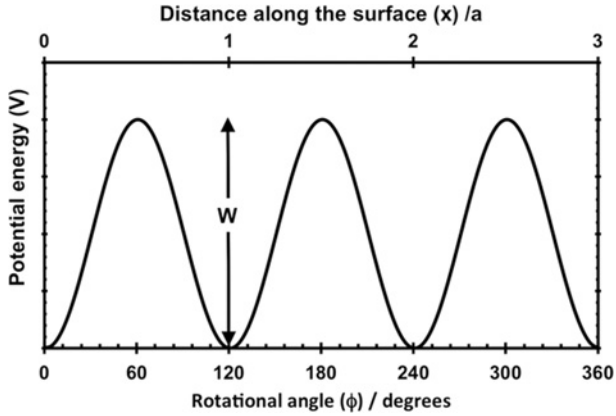


**Fig. 3.** Bottom axis: the classic hindered rotor: Potential energy *vs.* rotational angle for the rotation of one methyl group about the C–C axis in gas-phase ethane. From McQuarrie [11]. The same form of potential applies to helicopter-type rotations of an adsorbate. Top axis: potential energy *vs.* distance along the surface ($x$) for the diffusion of an adsorbate, where $a$ = site-to-site separation.

potential can be written:

$$V = (W/2)(1 - \cos n\varphi)\,, \tag{10}$$

where $W$ is the height of the potential barrier and $n$ is the number of equivalent minima in a full rotation (3 for Fig. 3). This potential gives a Schrödinger equation for motion that has been solved numerically, with the eigenvalues tabulated; and these have been used to compute the partition function and entropy *vs.* temperature [11,43]. Note that this potential looks like a HO near the energy minima and consequently has energy levels similar to those of a HO, with separations approximately given by $\varepsilon = (nh/2\pi)(W/2I)^{1/2}$, where $I$ is the reduced moment of inertia of the rotor. When the ratio $r = W/\varepsilon$ is huge, these equal the HO energies, but at lower $W/\varepsilon$ these have lower energy separations than $\varepsilon$.

Goddard's group [43] has calculated approximate analytical solutions for the eigenvalues and the partition function ($q$) for this hindered rotor problem *vs.* $W/\varepsilon$ and $kT/\varepsilon$, and has constructed a simple-to-calculate interpolation function, called the Hindered Rotor Density-of-States (HRDS) interpolation function, having these asymptotic forms. This HRDS function allows one to easily calculate $q$ and $S$ at any temperature for a potential energy function like Fig. 3 or the more general Eq. (10). One could easily calculate the partition function and entropy associated with the hindered rotations of adsorbates parallel to the surface using this HRDS approach, and get a far more accurate result than the harmonic approximation. Periodic DFT could be used to calculate estimates for the only three parameters in this model ($W$, $n$ and $I$) as described below. (Note that $\varepsilon$ is a simple function of these parameters.) Other efficient computational approaches have been used to estimate entropies of hindered internal rotations [44], and these could also be adapted to these helicopter-type rotations of adsorbates on surfaces. Note too that hindered internal rotations of adsorbates should also be treated

properly when $k_B T$ is not small compared to the barriers for these hindered internal rotations.

It might even be possible to apply the same HRDS approach to calculate the partition function and entropy associated with the translations of adsorbates parallel to the surface. Note that the potential energy of Fig. 3 and Eq. (10) for rotations parallel to the surface maps directly into that for adsorbate diffusion if we simply replace $n\varphi$ with $2\pi x/a$, where $x$ is distance and a is the site-to-site separation along the surface. Here $W$ is the diffusion barrier. If we replace $\varphi$ with $x$ and $I$ with mass ($m$), Schrödinger's equation has the same form (albeit with different boundary conditions), so one might be able to modify this HRDS approach [43] to estimate the partition function and entropy associated with such hindered translational motions of adsorbates as well. In this case, the high-temperature-limit entropy should resemble that of an ideal 2D gas instead of a free rotor. A closely related approach has already been proposed by Hill [45], which may be nearly as accurate. Again, DFT could be used to calculate the parameters in this modified-HRDS model or in Hill's model (*i.e.*, $a$ and $W$, with $\varepsilon$ being a simple function of $a$ and $W$.) As an example, our reported DFT calculations for water on Pt(111) give a diffusion barrier $W = 19$ kJ/mol and site-to-site separation $a = 0.28$ nm [46]. When fitted to cosine wave like Eq. (10), these give a second derivative at the minimum corresponding to a vibrational frequency of $\sim 67$ cm$^{-1}$, or $\sim 0.8$ kJ/mol excitation energy.

Note that many or even most of the adsorbates systems in Fig. 1 have attractive lateral interactions and exist mainly as 2D islands [5]. In the simplest model, this should lead to more restricted motions parallel to the surface. However, if one considers concerted motions of groups of adsorbates, this can lead to much smaller values of $W$, especially when the preferred adsorbate-adsorbate separation does not match the site-to-site separation on the lattice.

Now that we understand the origin of the empirical relationship in Fig. 1 and Eq. (1) between (high) adsorbate entropies and gas-phase entropies, we can predict that it will also hold for more strongly-bound adsorbates for the following reason. For a given surface, the barrier height $W$ for different adsorbates should increase roughly proportional to the desorption energy, $E_{des}$. The temperature ($T$) on Fig. 1 and Eq. (1) is limited to the range where desorption has the proper rate to perform equilibrium adsorption isotherm (EAI) and temperature-programmed desorption (TPD) measurements (*i.e.*, $\sim 10^{-3}$ to 100 monolayers/s). Thus, $T$ is also roughly proportional to $E_{des}$. So for the temperature range where Fig. 1 and Eq. (1) are expected to hold, $T/W$ is expected to be nearly independent of $E_{des}$, and it is this ratio that determines to what extent the system has approached the high-temperature limit. For a similar reason, Trouton's Rule is independent of the heat of vaporization, since it only applies at the normal boiling point, and this $T$ increases proportional to the heat of vaporization.

To test this expectation, Fig. 4 reproduces Fig. 2 but now also includes several experimental prefactors reported for more strongly bound adsorbates (CO, NO and Pb). The details of these new data points, which are for low coverages, are listed in Table 1. Except for the case of Pb at step edges on Mo(100), these data are also reasonably well predicted by Eq. (9), but on average it underestimates these by a factor of $\sim 3$. Table 1 is not nearly an exhaustive list of experimental prefactors for these species, but are representative and probably biased toward higher values than average. As noted pre-

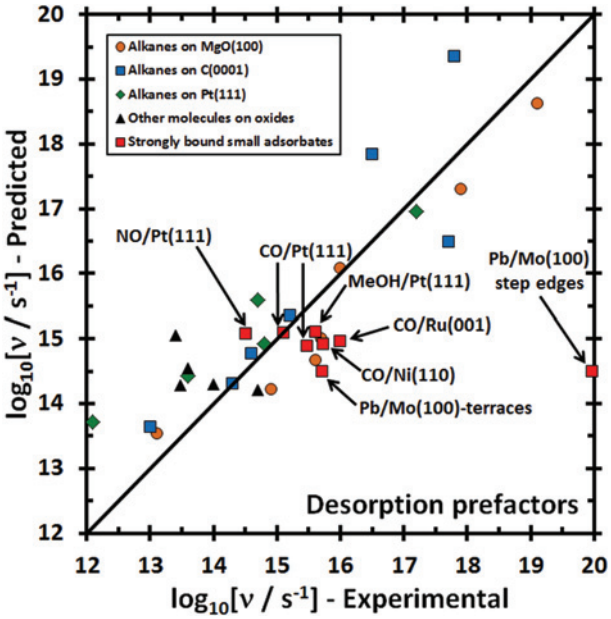


**Fig. 4.** Prefactors for the desorption of adsorbed species as predicted using Eq. (9) plotted *vs.* the experimentally measured prefactors. The line shows the expectation based on Eq. (9). Most of the data points were already shown in Fig. 2, but the new points (red squares) are for more strongly bound adsorbates (see Table 1 for details).

**Table 1.** Experimentally measured prefactors for desorption of strongly adsorbed small adsorbates and comparison to the predictions of Eq. (9).

| Adsorbate | Surface | $T$/K | $\log(\nu_{des}/s^{-1})$ experiment | $\log(\nu_{des}/s^{-1})$ from Eq. (9) | $S_{gas}(T)$ /R | $S_{ad}(T)$ /R | Citation |
|---|---|---|---|---|---|---|---|
| CO | Ru(001) | 477 | 16.0 | 15.0 | 25.4 | 12.1 | [9] |
| | Ni(110) | 435 | 15.7 | 14.9 | 25.1 | 12.4 | [48,49] |
| | Pt(111) | 410 | 15.5 | 14.9 | 24.9 | 12.7 | [50] |
| | Pt(111) | 600 | 15.1 | 15.1 | 26.2 | 15.0 | [51] |
| NO | Pt(111) | 575 | 14.5 | 15.1 | 26.2 | 16.4 | [52] |
| MeOH | Pt(111) | 210 | 15.6 | 15.1 | 27.1 | 14.5 | [29] |
| Pb | Mo(100) terraces | 1210 | 15.7 | 14.5 | 24.6 | 11.1 | [27] |
| | Mo(100) steps | 1210 | 20.0 | 14.5 | 24.6 | 1.3 | [27] |

viously [27], the energy barrier for Pb to detach from the step edges of Mo(100) is so high that it loses another degree on freedom (*i.e.*, surface diffusion away from the step edge) compared to Pb at terraces, so its entropy is much lower and its desorption prefactor is correspondingly 20,000-times larger. Similarly, the ratio $W/E_{des}$ should depend on the surface's atomic-scale corrugation with, for example, a larger $W/E_{des}$ ratio is expected for the (110) than (111) faces of FCC metals, so there may be some crystal

face dependence. A weak trend in this respect seems apparent in the data for CO on Ni surfaces [47].

At least from looking at the example of CO/Pt(111) from Table 1, it seems that HTST also greatly overestimates the desorption prefactor for these more strongly bound adsorbates. To estimate this, we used the vibrational frequencies for this system calculated by DFT reported by Greeley *et al.* for atop sites [53] except for the two lowest frequency modes, which were not reported. For these, we used the same group's reported DFT values for Cu(111) instead (193 and 194 $cm^{-1}$ [54]), which should be even smaller than on Pt since CO bonds more weakly to Cu. These give a prefactor in HTST at 600 K of $\sim 10^{19}$ $s^{-1}$, which is larger than the experimental values by a factor of $\sim 10^4$.

We repeat that Fig. 1 and Eq. (9) only hold at temperatures high enough for desorption rates to exceed $\sim 10^{-3}$ ML/s (*i.e.*, where $\tau$ is less than $\sim 1000$ s). At some point, the adsorbate entropy will decrease and the prefactor will increase as temperature is lowered such that $k_B T$ is much less than $W$.

## 5. Estimating prefactors for other elementary surface reactions

We now estimate prefactors for other elementary surface reactions using the qualitative picture of the potential energy surface for individual adsorbates in Fig. 3 together with the limiting case entropy represented by Eq. (1) and Fig. 1, which applies when the temperature is high enough for desorption to be observed in EAI or TPD measurements. Again, this is for terrace sites only since species at step edges have much lower entropies.

### 5.1 Adsorbate diffusion

Within TST, the rate constant for adsorbate diffusion is given by:

$$k_{\text{diff}} = (k_B T/h)\left(q^0_{TS}/q^0_i\right) \exp\left(-\Delta E^0_{TS}/k_B T\right), \tag{11}$$

where $q^0_{TS}$ is the partition function for the transition state (omitting one mode of motion along the reaction coordinate) and $q^0_i$ is the partition function for the adsorbate. The superscript "0" in both cases means that these are both evaluated about their zero-point energies (*i.e.*, taking all energies relative to the ground state for that species), and $\Delta E^0_{TS}$ is the difference between these two zero-point energies. To be most rigorous, one would plot $\ln(k_{\text{diff}})$ *vs.* $1/T$ to get the activation energy ($E_{\text{act}}$ = the slope at the temperature of interest times $-$R) and the prefactor $\nu_{\text{diff}}$ (where $\ln(\nu_{\text{diff}})$ = the $y$-intercept). Both will vary slowly with $T$. Alternatively, one can get the prefactor from $\nu_{\text{diff}} = k_B T/h \exp[(S^0_{TS,\text{diff}} - S^0_{\text{ad}})/\text{R}]$, where both entropies are evaluated at the temperature of interest. As noted above, within HTST, the entropy of both species is calculated from the sum over all vibrational modes of $\text{R}\{(h\nu_i/kT)/[\exp(h\nu_i/kT) - 1] - \ln[1 - \exp(-h\nu_i/kT)]\}$ . For simplicity, $\nu_{\text{diff}}$ is often approximated as $(k_B T/h)(q^0_{TS}/q^0_i)$, with $E_{\text{act}}$ approximated as $\Delta E^0_{TS}$. This is not as accurate as these other two methods for calculating either separate value ($\nu_{\text{diff}}$ or $E_{\text{act}}$), but their combination obtained in this way at any temperature gives the correct rate constant.

Diffusion rates are usually measured at temperatures where $k_B T$ is very small compared to the barriers in Fig. 3 for motion parallel to the surface. In this case, HTST should be accurate, wherein both $q^0_{TS}$ and $q^0_i$ are pure vibrational partition functions. Note that this is for temperatures far below those where Fig. 1 and Eq. (1) are valid, since those are valid only when desorption rates are fast enough to measure (which requires much higher temperature than diffusion for the same adsorbate). Thus HTST has been used, for example, together with embedded atom potentials to calculate the barrier, fundamental vibrational frequencies and prefactor for diffusion of Cu on Cu(100), and this gave good agreement with experimental results [55]. We used it together with energetics and vibrational frequencies calculated using DFT with periodic boundary conditions to calculate the prefactors for the diffusion of small $Pd_n$ clusters ($n = 1$ to 4) on MgO(100) [56]. The values at 250 K were in the range $\sim 10^{11}$ to $10^{14}$ $s^{-1}$, with the tetramer having a prefactor 100- to 1000-fold larger than the monomer and dimer, due to a "floppy" transition state.

It is possible that some adsorbates might have relatively free rotations parallel to the surface while $k_B T$ is still very small compared to the barrier for diffusion. In these cases, it is unlikely that the partition function for these rotations will be much different between the adsorbed state and its transition state for diffusion, so the rotational contributions will nearly cancel. Hence, HTST should still offer a reasonable approximation for $\nu_{diff}$.

If one is trying to predict diffusion rates at much higher temperatures (*i.e.*, where desorption rates are fast enough to measure), then HTST is no longer valid. Instead, the entropies for the initial state and the transition state should both be much larger than the vibrational entropies and similar to the entropy given by Eq. (1). Keeping this in mind, the ratio $q^0_{TS}/q^0_i$ in Eq. (1) can be estimated by recognizing that $q^0_{TS}$ and $q^0_i$ will be very similar except that $q^0_{TS}$ is missing one translational mode (the reaction coordinate for diffusion). The entropy for this translational mode, $S^0_{gas,1D\text{-}trans}$, can be calculated using Eq. (4), and the prefactor is given by:

$$\nu_{diff} = k_B T/h \exp\left(-S^0_{gas,1D\text{-}trans}/R\right). \tag{12}$$

This is much smaller than the value that would be predicted by Eq. (11) using HTST, which reflects the increasing contribution to the initial adsorbate's partition function from its motion in the direction of the reaction coordinate (*i.e.*, motion in the direction of diffusion) with increasing temperature. Note that this contribution is <u>not</u> included in the partition function of the transition state.

### 5.2 Adsorbate dissociation

Consider an adsorbate's dissociation reaction of the type:

$$AB_{ad} \rightleftharpoons AB_{ad,TS} \rightarrow A_{ad} + B_{ad}\,, \tag{13}$$

where $AB_{ad,TS}$ is the transition state. We have previously tabulated a list of 25 values of the prefactor for the dissociation of different adsorbates on different single crystal surfaces [28]. Those values showed a clear trend in that the prefactor for dissociation

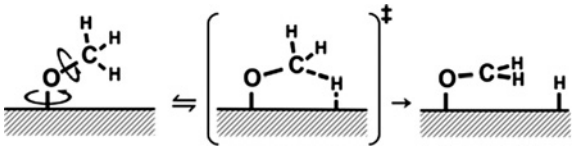

**Fig. 5.** Schematic representation showing how entropy is lost in the transition state for the dissociation of an adsorbate, in this example for an adsorbed methoxy on a metal surface losing a methyl H to form adsorbed -$OCH_2$ plus $H_{ad}$. The reactant has two relatively free rotations, but those motions are lost as the methyl starts to form its own bond to the metal in the transition state.

($\nu_{diss}$) was only $1/10$ to $1/10^5$ of the prefactor for desorption ($\nu_{des}$) of the same molecule at the same temperature, with an average ratio ($\nu_{diss}/\nu_{des}$) of $\sim 1/1000$. (This was for low coverages where both reactions were assumed to be first-order in coverage.) In that work, the main emphasis was on this ratio of prefactors rather than the absolute value for $\nu_{diss}$, since the latter was usually only determined by multiplying the experimentally measured ratio by some assumed value of $\nu_{des}$, typically $10^{13}$ $s^{-1}$ which we showed above can be many orders of magnitude too low (Fig. 2). A recent experimental study of the kinetic competition between dissociation and desorption of propane on PdO(101) also shows a ratio $\nu_{diss}/\nu_{des}$ of $\sim 1/1000$, that was also reproduced by DFT calculations when the extra entropy of the adsorbates mentioned above was approximately included [63].

The low value for the ratio $\nu_{diss}/\nu_{des}$ can be understood as follows. If a relatively freely moving part of the adsorbate starts forming a new bond to the surface in the transition state, the partition function of this three-center transition state will naturally be smaller than that of the reactant. An example is shown in Fig. 5, where adsorbed methoxy on a metal surface (metal-$OCH_3$) loses a methyl H to form adsorbed -$OCH_2$ plus $H_{ad}$. In the reactant, the methyl could be nearly a free rotor both around its own central axis of symmetry and around the metal-O bond axis, but those motions are lost as the methyl starts to form its own bond to the metal in the transition state. This effect is analogous to the situation in gas-phase or solution-phase reactions where the partition function is generally lowered when forming transition states with reduced rotational entropy [14,57]. For a similar reason, the cyclization of a linear gas molecule generally leads to a decrease in entropy.

The simplest approach to estimating $\nu_{diss}$ for dissociation of adsorbates is to multiply the value of $\nu_{des}$ for the same molecule, estimated from Eq. (9), by this average ratio of $10^{-3}$ mentioned above:

$$\nu_{diss} = \sim 10^{-3}\nu_{des} \,. \tag{14}$$

Since dissociation rates for molecular adsorbates are usually measured in the same temperate range as desorption rates, using Eq. (9) for $\nu_{des}$ is treating its behavior in the proper temperature regime. However, this is often not true for non-molecular adsorbates (*i.e.*, molecular fragments) like the methoxy species shown in Fig. 5, which would have a much higher desorption temperature (to make a methoxy radical) than the temperatures where it is typically seen to dissociate (*i.e.*, one often wants to evaluate $\nu_{diss}$ at temperatures where the surface residence time exceeds $\sim 1000$ s). For the dissociation

of such adsorbed molecular fragments, it may be better to estimate $\nu_{des}$ (or $\nu_{diss}$ directly) using HTST. One must do something like what is recommended in Section 4 above to get partition functions or entropies that would be more generally accurate.

### 5.3 Association of two adsorbates

Consider the association reaction of two adsorbates of the type:

$$A_{ad} + B_{ad} \rightleftharpoons AB_{ad,TS} \rightarrow AB_{ad}, \tag{15}$$

where $AB_{ad,TS}$ is again the transition state. The standard entropy change for this net reaction, $\Delta S^0_{ass}$, must equal the sum of $\Delta S^0_{step}$ for the two elementary steps in Reaction (15) above:

$$\Delta S^0_{ass} = \Delta S^0_{step1} + \Delta S^0_{step2} = \Delta S^0_{TS,ass} - \Delta S^0_{TS,diss}\,, \tag{16}$$

where $\Delta S^0_{TS,diss}$ is the standard entropy of activation for dissociation Reaction (13), which is the reverse of this association Reaction (15). Here we have used the fact that $\Delta S^0_{step2} = -\Delta S^0_{TS,diss}$. Dividing both sides by R and then taking the exponential of both sides gives:

$$\begin{aligned}\exp\left(\Delta S^0_{ass}/\mathrm{R}\right) &= \exp\left(\Delta S^0_{TS,ass}/\mathrm{R} - \Delta S^0_{TS,diss}/\mathrm{R}\right)\\ &= \exp\left(\Delta S^0_{TS,ass}/\mathrm{R}\right)/\exp\left(\Delta S^0_{TS,diss}/\mathrm{R}\right).\end{aligned} \tag{17}$$

Since $\nu_i = k_B T/h \exp(\Delta S^0_{TS,i}/\mathrm{R})$ for each step $i$, the ratio on the right side of this expression is just $\nu_{ass}/\nu_{diss}$, so that:

$$\nu_{ass} = \nu_{diss} \exp\left(\Delta S^0_{ass}/\mathrm{R}\right) = \nu_{diss} \exp\left[\left(S^0_{AB,ad} - S^0_{A,ad} - S^0_{B,ad}\right)/\mathrm{R}\right]. \tag{18}$$

One can estimate $\nu_{ass}$ using Eq. (18) by getting $\nu_{diss}$ using the method described in the previous section and getting $S^0_{i,ad}$ for each adsorbed species $i$ ($A$, $B$ and $AB$) from Fig. 1 or Eq. (1). Obtaining any adsorbate's entropy using Fig. 1 or Eq. (1) requires knowing its standard gas-phase entropy at the same temperature, which is easy to estimate [11, 12] by extrapolating from tabulated entropies at similar conditions using tabulated heat capacities (such as the NIST tables of thermodynamic data).

One cannot use Fig. 1 to estimate the entropy for adsorbed $A$ or $B$ in this application if one is studying the rate of their association reaction at a temperature far below its desorption temperature, since Fig. 1 is only known to be valid for temperatures where the desorption rate is at least $10^{-3}$ ML/s ($\tau < \sim 1000$ s). For example, a prefactor of $10^{17}$ $s^{-1}$ was determined experimentally for the associative desorption of water from adsorbed -OH plus -H on $\alpha$-$Fe_2O_3$(012) (1 × 1) [58]. This prefactor is higher than that for desorption of molecularly adsorbed water, and higher than would be expected based on the above analysis. This was attributed to the expectation that at the low temperature of that study, most of the translational and rotational motion of these adsorbed fragments (-OH and -H) have probably been frozen out into vibrational modes, thus lowering their entropy below that predicted by Fig. 1 [59]. At such temperatures, standard HTST should be valid.

## 6. Dealing with mechanistic complexity: when an adsorbate must assume some special minority structure before producing the transition state

In surface reactions, it is very common for the adsorbate in its dominant form on the surface to first convert to some minority species before producing the transition state for the types of reactions discussed above. For example, for most of the desorption reactions in Fig. 2, the dominant form of the adsorbate is in 2D islands, yet at coverages below 50% of saturation, it probably desorbs by first detaching from the islands to make adsorbed monomers (as a dilute 2D lattice gas or ideal 2D gas), and then desorbing from this dilute state. Similarly, association reactions often occur by a mechanism where one species is in islands and the other diffuses up to populate a special site at the edge of those islands (where it may be much less stable in energy than as an isolated monomer at a site well separated from island). Also, dissociation reactions for adsorbates often happen mainly at defect sites.

How does one relate the rates for such processes that involve minority structures for an adsorbate to the coverage of the dominant state of that adsorbate, which is usually the only type of coverage that one can actually measure? One of the beauties of TST is that its derivation requires thermal equilibrium between the reactants and transition state. Thus, it does not matter how many intermediate states there are between the measureable reactants and the transition state, if they are also in equilibrium with the reactants one arrives at the same rate expression. Thus, one only needs to be able to fully describe the measureable reactants and the transition state to use its results. For example, consider the association reaction of two adsorbates of the type originally considered in Reaction (15) above, but let us now add the mechanistic complexity that the dominant form of reactant $A$ is now in islands ($A_{\mathrm{ad,dominant}}$), but that it must be in some special minority form ($A_{\mathrm{ad,special}}$), like an isolated monomer or at some defect site, before it can react with $B_{\mathrm{ad}}$:

$$A_{\mathrm{ad,dominant}} + B_{\mathrm{ad}} \rightleftharpoons A_{\mathrm{ad,special}} + B_{\mathrm{ad}} \rightleftharpoons AB_{\mathrm{ad,TS}} \rightarrow AB_{\mathrm{ad}}. \tag{19}$$

As long as $A_{\mathrm{ad,dominant}}$ is in equilibrium with $A_{\mathrm{ad,special}}$, one can ignore this intermediate state in deriving the TST rate expression, and one still arrives at the same result. Since surface migration processes are often so fast compared to the rate-controlling step(s) in the overall surface reaction mechanism, it is often safe to assume that the equilibrium $A_{\mathrm{ad,dominant}} \rightleftharpoons A_{\mathrm{ad,special}}$ is fast enough to apply this. For example, in catalytic reactions, the rate-controlling steps usually have much larger activation energies than surface migration steps. Also, this assumption is particularly likely to be true under steady-state reaction conditions where the surface coverages of all species are constant. Of course, if the transition state is at some special site like a defect, one must take this into consideration in describing the nature (energy and partition function) for the transition state, but one need not know how to describe $A_{\mathrm{ad,special}}$ in any detail, or even know that it exists.

## 7. Statistical models for adsorbates: 2D ideal gas, 2D lattice gas and 2D crystals

Surface chemists usually think about the statistical mechanics of adsorbates in terms of the two limiting cases that have been discussed in statistical thermodynamics

texts: the 2D ideal gas model and the 2D lattice gas model, with or without lateral adsorbate-adsorbate interactions [45] (for more sophisticated models and applications, see also [6–8]). If adsorbates have attractive interactions and form large 2D islands, one can also treat them as perfect 2D crystals. Depending on which model is used to represent each adsorbate, one gets different expressions for the rate constant and the coverage dependence of the rate using transition state theory. These differences arise entirely through the different expressions one gets when calculating the concentration of the transition state assuming it is in equilibrium with the reactants, as shown below.

Consider again Reaction (15), the association of two adsorbates:

$$A_{ad} + B_{ad} \rightleftharpoons AB_{ad,TS} \rightarrow AB_{ad}. \tag{15}$$

If adsorbed $A$, $B$ and the transition state are all ideal 2D gases, the TST rate for Reaction (15), $r_{ass}$, is:

$$r_{ass} = k_{ass} C_A C_B \tag{20}$$

where $C_i$ is the concentration of adsorbed $i$ (in moles per unit area) and $k_{ass}$ is the rate constant in units of (moles per area × time)$^{-1}$, so that $r_{ass}$ has units of (moles $AB$ produced per area per time). By equating the chemical potential of $AB_{ad,TS}$ with the sum of the chemical potentials for $A_{ad} + B_{ad}$ (*i.e.*, the equilibrium criterion), the rate constant in TST can be shown to equal:

$$k_{ass} = N_A (k_B T/h) \left\{ \left(q^0_{TS}/A\right) \Big/ \left[ \left(q^0_A/A\right)\left(q^0_B/A\right) \right] \right\} \exp\left(-\Delta E^0_{TS}/k_B T\right), \tag{21}$$

where $q^0_i/A$ is the molecular partition function per unit area for each species i evaluated about its own zero-point energy (*i.e.*, taking its zero-point energy as energy = 0), and $\Delta E^0_{TS}$ is the difference in zero-point energy between the reactants and transition state. Note that $q^0_{TS}$ has a special definition in that one must remove from it one degree of freedom (the reaction coordinate's contribution, which is related to the $A$-$B$ stretching vibration of the product $AB$). (As usual in the derivation of the TST rate, this contribution cancels with a factor in the rate at which the transition state itself converts to products.) Such removal also applies to all its uses below. Since all three partition functions in Eq. (17) include two degrees of translational motion, their values are proportional to area $A$, and so $A$ cancels out in $k_{ass}$. Its prefactor-like product $N_A(k_B T/h)\{(q^0_{TS}/A)/[(q^0_A/A)(q^0_B/A)]\}$ will usually be much, much less than $N_A(k_B T/h) = \sim N_A(10^{13}\ s^{-1})$ since this ratio of $q$ values includes two more degrees of translational motion in its denominator.

If $A$, $B$ and TS are all treated instead as ideal (*i.e.*, non-interacting) 2D lattice gases, the TST rate for Reaction (17) is:

$$r_{ass,LG} = k_{ass,LG}[\theta_A/(1-\theta_A)][\theta_B/(1-\theta_B)], \tag{22}$$

where $\theta_i$ is the fractional occupation of sites by adsorbed $i$ (unitless) and $k_{ass,LG}$ is the rate constant in units of time$^{-1}$, so that $r_{ass}$ has units of time$^{-1}$ (which really means monolayers converted per unit time). (This equation assumes that $A$ and $B$ use different, independent sites. If $A$ and $B$ compete for the same sites, which is more likely, the

denominators here should both be changed to $(1-\theta_{\text{total}})$, where $\theta_{\text{total}}$ is the total coverage of all adsorbates.) The rate constant in TST is:

$$k_{\text{ass,LG}} = (k_B T/h)\left[q^0_{TS}/\left(q^0_A q^0_B\right)\right] \exp\left(-\Delta E^0_{TS}/k_B T\right), \tag{23}$$

where $q^0_i$ is the molecular partition function for each species $i$ evaluated about its own zero-point energy, and $\Delta E^0_{TS}$ is the difference in zero-point energy between the reactants and transition state. Again, these equations can be derived by equating the chemical potential of $AB_{\text{ad,TS}}$ with the sum of the chemical potentials for $A_{\text{ad}} + B_{\text{ad}}$ (*i.e.*, assuming equilibrium), with an identical derivation to that above except for the difference in the expressions for the chemical potentials of ideal 2D lattice gases *vs.* ideal 2D gases. Note that $q^0_i$ has only vibrational contributions at low temperature, but the adsorbate might be a hindered rotor or even free rotor in its lattice site at higher temperatures, but still not so high that the lattice site model breaks down.

The unusual $1/(1-\theta_i)$ factors in this rate expression arise because the chemical potential of i includes the term $k_B T \ln[\theta_i/(1-\theta_i)]$ in the ideal 2D lattice gas model, which increases with $\theta_i$ below ½ monolayer but decreases above that, due to the configurational entropy of the adsorbate [45].

If one derives the rate expression for desorption of molecularly adsorbed species for cases where the sticking probability is near unity (*i.e.*, non-activated adsorption, like the situations treated in Section 3 above), TST gives that the rate of desorption is also proportional to $\theta/(1-\theta)$ for the ideal lattice gas model. This arises from equating the chemical potential of the adsorbed 2D lattice gas (which includes $k_B T \ln[\theta/(1-\theta)]$) with that for the transition state (an ideal 2D gas). The sharp decrease in activation energy for desorption ($E_d$) with increasing coverage near saturation so commonly seen as $\theta$ approaches 1 when rates are analyzed as proportional to $\theta_i$ as in Eq. (2) instead of $\theta/(1-\theta)$ is at least partly an artifact of omitting this $(1-\theta)$ in the denominator. Similarly, the exponential increase in apparent prefactor for desorption with coverage reported for some cases [6] can be attributed at least partially to neglecting this. Note that we cancelled the $1/(1-\theta_{TS})$ factor in the derivation of this rate expression for association above, since it is safe to assume that the coverage of the transition state is so low that this factor equals unity. Note too that this $\theta/(1-\theta)$ factor leads properly to the first-order Langmuir adsorption isotherm relating $\theta$ to gas pressure when derived using equilibrium thermodynamics [45], and it is also easily derived from kinetics by setting this desorption rate equal to the adsorption rate for this case where the sticking probability ($S$) is 1 at all coverages. This derivation gives the same result as the more common kinetic derivation which assumes the desorption rate is proportional instead to $\theta$ and $S$ is proportional to $(1-\theta)$, but conceptually it is quite different. When measured carefully, sticking probabilities are often observed to be very close to unity right up to saturation, with the apparent decrease in long-term sticking probability above 90% of saturation coverage actually due to desorption of transiently adsorbed species [29,60–62]. This $\theta/(1-\theta)$ factor in the desorption rate expression fully explains their short lifetimes on the surface at such high coverages: new sites or strongly repulsive lateral interactions are not needed to qualitatively explain such observations.

Returning to the case of associative desorption, Reaction (15), if we assume that $A$ and $B$ are both 2D crystal islands (*i.e.*, are lattice gases but have attractive interactions

so they reside in larger, perfect 2D islands of pure $A$ and pure $B$), but that TS is still a lattice gas, then the coverage dependence drops completely out of the rate expression in Eq. (18). In this case, the rate simply equals the rate constant ($r_{\mathrm{ass,crystal}} = k_{\mathrm{ass,crystal}}$), where the rate constant $k_{\mathrm{ass,crystal}}$ equals $k_{\mathrm{ass,LG}}$, the same expression as Eq. (20).

If one must use different models for the two adsorbates (*e.g.*, ideal 2D gas for $A$ and ideal 2D lattice gas for $B$), derivation of the TST rate expression starting with the equilibrium assumption again shows that one can still calculate the rate constant using Eq. (23) but one must replace $q_{\mathrm{i}}^0$ with $q_{\mathrm{i}}^0/(N_{\mathrm{A}}A)$ for every species that is treated as an ideal 2D gas. In the rate expression, Eq. (22), one must also replace $\theta_{\mathrm{i}}/(1-\theta_{\mathrm{i}})$ with $C_{\mathrm{i}}$ for every reactant species that is treated as an ideal 2D gas. One must take the units on $N_{\mathrm{A}}$ to be mole$^{-1}$ so that the units work, with the rate having units of moles produced per area per s, or s$^{-1}$ (*i.e.*, monolayer per s), depending on whether the transition state is treated as an ideal 2D lattice gas or ideal 2D gas.

## 8. Conclusions

Our recent discovery of a correlation between adsorbate entropies and gas-phase entropies (Fig. 1) provides a powerful new approach presented here for estimating kinetic prefactors for surface reactions involving desorption, diffusion, dissociation and association of adsorbates, provided the temperature is high enough that the adsorbate's surface residence time is less than $\sim 1000$ s. At these temperatures, HTST does very poorly at predicting such prefactors, but at temperatures where $k_{\mathrm{B}}T$ is small compared to the barriers $W$ (Fig. 3) for adsorbate diffusion and helicopter-type rotation, HTST is more accurate. At intermediate temperatures where $k_{\mathrm{B}}T$ approaches $W$, a new approach must be developed, and we offer here a suggestion for that approach that can be adopted from the methods used to treat hindered internal rotations of gas molecules. Whereas the rates of adsorbates' reactions are usually treated as being first-order in adsorbate coverage ($\theta$), transition state theory shows that it is better to use $\theta/(1-\theta)$ as the "concentration" factor (when not 2D islands), since it more accurately reflects the tremendous increase in the adsorbate's chemical potential as coverage approaches saturation due to the configurational entropy or excluded volume effect.

### Acknowledgement

The authors gratefully acknowledge support for this work by the National Science Foundation under CHE-1010287 and the DOE-OBES under grant #DE-FG02-96ER14630, and Prof. Hannes Jónsson for computational time on Gardar, the Nordic high performance computing center. We thank Lars C. Grabow, Robert J. Madix, Jason F. Weaver and the reviewers for very insightful discussions and comments on this manuscript.

### References

1. H. Eyring and M. Polanyi, Z. Phys. Chem. B-Chem. E., **12** (1931) 279.
2. G. Henkelman, B. P. Uberuaga, and H. Jonsson, J. Chem. Phys. **113** (2000) 9901.
3. A. Heyden, A. T. Bell, and F. J. Keil, J. Chem. Phys. **123** (2005) 224101.
4. G. Henkelman and H. Jonsson, J. Chem. Phys. **115** (2001) 9657.

5. C. T. Campbell and J. R. V. Sellers, J. Am. Chem. Soc. **134** (2012) 18109.
6. K. J. Wu and S. D. Kevan, J. Chem. Phys. **95** (1991) 5355.
7. L. D. Peterson and S. D. Kevan, Phys. Rev. Lett. **65** (1990) 2563.
8. S. H. Payne, J. S. McEwen, H. J. Kreuzer, and D. Menzel, Surf. Sci. **594** (2005) 240.
9. H. Pfnur, P. Feulner, H. A. Engelhardt, and D. Menzel, Chem. Phys. Lett. **59** (1978) 481.
10. R. J. Madix, G. Ertl, and K. Christmann, Chem. Phys. Lett. **62** (1979) 38.
11. D. A. McQuarrie, *Statistical Mechanics*, University Science Books, Sausalito (2000).
12. P. Atkins, *Physical Chemistry*, 6th edn., W. H. Freeman, New York (1998), Chapts. 27 and 4.
13. W. A. Brown, R. Kose, and D. A. King, Chem. Rev. **98** (1998) 797.
14. K. J. Laidler, *Chemical Kinetics*, 2nd edn., McGraw-Hill, New York (1965).
15. A. J. Gellman and K. R. Paserba, J. Phys. Chem. B **106** (2002) 13231.
16. K. R. Paserba and A. J. Gellman, J. Chem. Phys. **115** (2001) 6737.
17. K. R. Paserba, N. Vaidyanathan, and A. J. Gellman, Langmuir **18** (2002) 9799.
18. S. L. Tait, Z. Dohnalek, C. T. Campbell, and B. D. Kay, J. Chem. Phys. **122** (2005) 164708.
19. S. L. Tait, Z. Dohnalek, C. T. Campbell, and B. D. Kay, J. Chem. Phys. **125** (2006) 234308.
20. K. A. Fichthorn, K. E. Becker, and R. A. Miron, Catal. Today **123** (2007) 71.
21. K. E. Becker and K. A. Fichthorn, J. Chem. Phys. **125** (2006) 184706.
22. K. E. Becker, M. H. Mignogna, and K. A. Fichthorn, Phys. Rev. Lett. **102** (2009) 046101.
23. S. J. Lombardo and A. T. Bell, Surf. Sci. Rep. **13** (1991) 1.
24. H. Sellers and J. Gislason, Surf. Sci. **426** (1999) 147.
25. M. L. Wise, B. G. Koehler, P. Gupta, P. A. Coon, and S. M. George, Surf. Sci. **258** (1991) 166.
26. V. P. Zhdanov, Surf. Sci. Rep. **12** (1991) 183.
27. D. E. Starr and C. T. Campbell, J. Am. Chem. Soc. **130** (2008) 7321.
28. C. T. Campbell, Y.-K. Sun, and W. H. Weinberg, Chem. Phys. Lett. **179** (1991) 53.
29. E. M. Karp, T. L. Silbaugh, M. C. Crowe, and C. T. Campbell, J. Am. Chem. Soc. **134** (2012) 20388.
30. G. Kresse and J. Hafner, Phys. Rev. B **47** (1993) 558.
31. G. Kresse and J. Hafner, Phys. Rev. B **49** (1994) 14251.
32. G. Kresse and J. Furthmuller, Comp. Mater. Sci. **6** (1996) 15.
33. G. Kresse and D. Joubert, Phys. Rev. B **59** (1999) 1758.
34. P. E. Blochl, Phys. Rev. B **50** (1994) 17953.
35. J. P. Perdew, J. A. Chevary, S. H. Vosko, K. A. Jackson, M. R. Pederson, D. J. Singh, and C. Fiolhais, Phys. Rev. B **46** (1992) 6671.
36. J. P. Perdew, K. Burke, and M. Ernzerhof, Phys. Rev. Lett. **77** (1996) 3865.
37. J. P. Perdew, K. Burke, and M. Ernzerhof, Phys. Rev. Lett. **78** (1997) 1396.
38. J. Greeley and M. Mavrikakis, J. Am. Chem. Soc. **124** (2002) 7193.
39. M. W. Chase Jr., J. Phys. Chem. Ref. Data **1998**, Monograph 9, 1.
40. J. C. Hamilton, Phys. Rev. Lett. **77** (1996) 885.
41. P. Atkins, *Physical Chemistry*, 6th edn., W. H. Freeman & Company, New York (1998), p. 106.
42. A. Antony, A. Asthagiri, and J. F. Weaver, Phys. Chem. Chem. Phys. **14** (2012) 12202.
43. R. B. McClurg, R. C. Flagan, and W. A. Goddard, J. Chem. Phys. **106** (1997) 6675.
44. A. Ghysels, T. Verstraelen, K. Hemelsoet, M. Waroquier, and V. Van Speybroeck, J. Chem. Inf. Model. **50** (2010) 1736.
45. T. L. Hill, *An Introduction to Statistical Thermodynamics*, Addison-Wesley, Reading, MA (1960).
46. L. Arnadottir, E. M. Stuve, and H. Jonsson, Surf. Sci. **606** (2012) 233.
47. J. T. Stuckless, Al-N. Sarraf, C. Wartnaby, and D. A. King, J. Chem. Phys. **99** (1993) 2202.
48. C. R. Helms and R. J. Madix, Surf. Sci. **52** (1975) 677.
49. J. L. Falconer and R. J. Madix, Surf. Sci. **48** (1975) 393.
50. J. S. McEwen, S. H. Payne, H. J. Kreuzer, M. Kinne, R. Denecke, and H. P. Steinruck, Surf. Sci. **545** (2003) 47.
51. C. T. Campbell, G. Ertl, H. Kuipers, and J. Segner, Surf. Sci. **107** (1981) 207.
52. C. T. Campbell, G. Ertl, and J. Segner, Surf. Sci. **115** (1982) 309.
53. J. Greeley and M. Mavrikakis, J. Am. Chem. Soc. **126** (2004) 3910.
54. L. C. Grabow and M. Mavrikakis, ACS Catal. **1** (2011) 365.

55. U. Kürpick, A. Kara, and T. S. Rahman, Phys. Rev. Lett. **78** (1997) 1086.
56. L. J. Xu, G. Henkelman, C. T. Campbell, and H. Jonsson, Phys. Rev. Lett. **95** (2005) 146103.
57. D. G. Trular, A. D. Isaacson, and B. C. Garrett, Generalized Transition State Theory, in: *Theory of Chemical Reactions*, M. Baer (Ed.), CRC Press: Boca Raton (1985), Vol. IV, 65–137.
58. M. A. Henderson, S. A. Joyce, and J. R. Rustad, Surf. Sci. **417** (1998) 66.
59. C. T. Campbell and J. R. V. Sellers, Chem. Rev. **113** (2013) 4106.
60. J. M. Gottfried, E. K. Vestergaard, P. Bera, and C. T. Campbell, J. Phys. Chem. B **110** (2006) 17539.
61. O. Lytken, W. Lew, J. J. W. Harris, E. K. Vestergaard, J. M. Gottfried, and C. T. Campbell, J. Am. Chem. Soc. **130** (2008) 10247.
62. H. Ihm, H. M. Ajo, and C. T. Campbell, J. Phys. Chem. B **108** (2004) 14627.
63. A. Anthony, A. Asthagiri, and J. F. Weaver, Phys. Chem. Chem. Phys. **14** (2012) 12202.